Design and fabrication of two-dimensional semiconducting bolometer arrays for the High resolution Airborne Wideband Camera (HAWC) and the Submillimeter High Angular Resolution Camera II (SHARC-II)

George M. Voellmer*[a], Christine A. Allen[a], Michael J. Amato[a], Sachidananda R. Babu[a]; Arlin E. Bartels[a], Dominic J. Benford[a], Rebecca J. Derro[a], C. Darren Dowell[b]; D. Al Harper[c]; Murzy D. Jhabvala[a]; S. Harvey Moseley[a]; Timothy Rennick[c]; Peter J. Shirron[a]; W. Wayne Smith[d]; Johannes G. Staguhn[e]

[a]NASA Goddard Space Flight Center; [b]California Institute of Technology; [c]University of Chicago; [d]OSC/GSFC; [e]SSAI/GSFC

ABSTRACT

The High resolution Airborne Wideband Camera (HAWC) and the Submillimeter High Angular Resolution Camera II (SHARC II) will use almost identical versions of an ion-implanted silicon bolometer array developed at the National Aeronautics and Space Administration's Goddard Space Flight Center (GSFC). The GSFC "Pop-Up" Detectors (PUD's) use a unique folding technique to enable a 12 x 32-element close-packed array of bolometers with a filling factor greater than 95 percent. A kinematic Kevlar® suspension system isolates the 200 mK bolometers from the helium bath temperature, and GSFC – developed silicon bridge chips make electrical connection to the bolometers, while maintaining thermal isolation. The JFET preamps operate at 120 K. Providing good thermal heat sinking for these, and keeping their conduction and radiation from reaching the nearby bolometers, is one of the principal design challenges encountered.

Another interesting challenge is the preparation of the silicon bolometers. They are manufactured in 32-element, planar rows using Micro Electro Mechanical Systems (MEMS) semiconductor etching techniques, and then cut and folded onto a ceramic bar. Optical alignment using specialized jigs ensures their uniformity and correct placement. The rows are then stacked to create the 12 x 32-element array.

Engineering results from the first light run of SHARC II at the CalTech Submillimeter Observatory (CSO) are presented.

1. INTRODUCTION

The High resolution Airborne Wideband Camera (HAWC) [1] and the Submillimeter High Angular Resolution Camera II (SHARC II)[2] are both far-infrared instruments being built to study star formation, protoplanetary disks, and interstellar gas and dust. HAWC will be a facility instrument for the Stratospheric Observatory for Infrared Astronomy, an airplane-based telescope, and SHARC will be a CSO facility instrument. Both will use almost identical versions of a 384-element bolometer array developed at the GSFC (Figs. 1&2). As of this writing, the SHARC-II detector has been built and successfully tested, and the HAWC parts fabrication has started.

*contact: voellmer@gsfc.nasa.gov ;Telephone: (301)-286-8182; Code 543 NASA / GSFC, Greenbelt, MD 20771

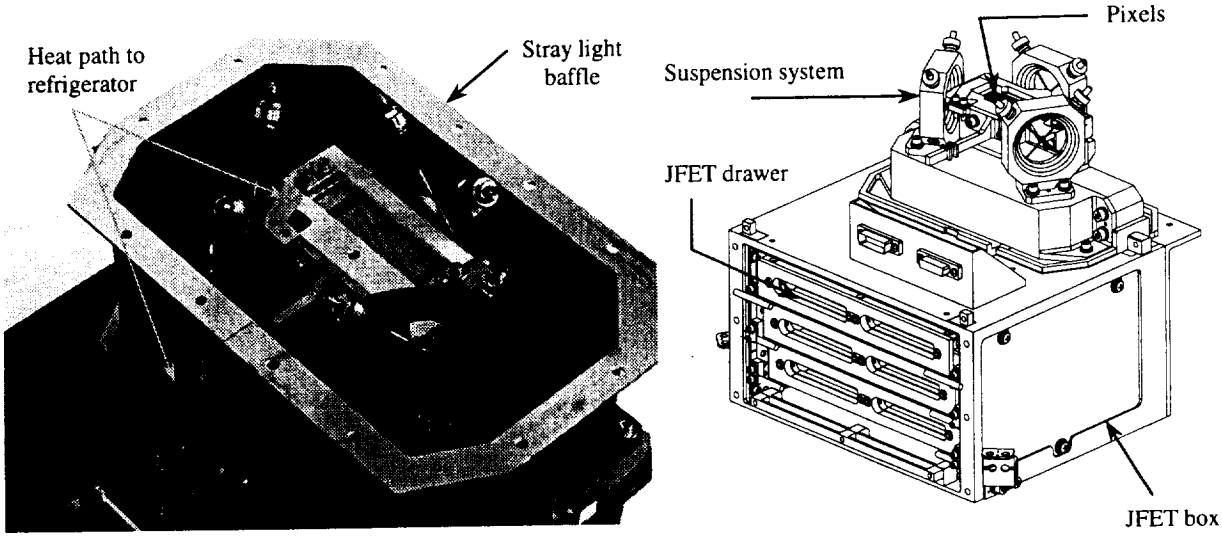

Fig.s 1&2: The SHARC detector

2. DETECTOR MECHANICAL DESIGN

The core of the detector (Figs. 3&4) consists of a stack of 12 ceramic printed circuit boards, or "fanout boards", each with a folded, 32-element, linear PUD bolometer array arranged on one edge, and a JFET "drawer" extending orthogonally from one face.

Structurally, the fanout boards are glued into a titanium strongback. The bolometer assemblies are glued into a ceramic holder, the "upper C". The upper C is attached to the strongback with a Kevlar suspension system. The JFET drawers are held in a box, to which the strongback attaches.

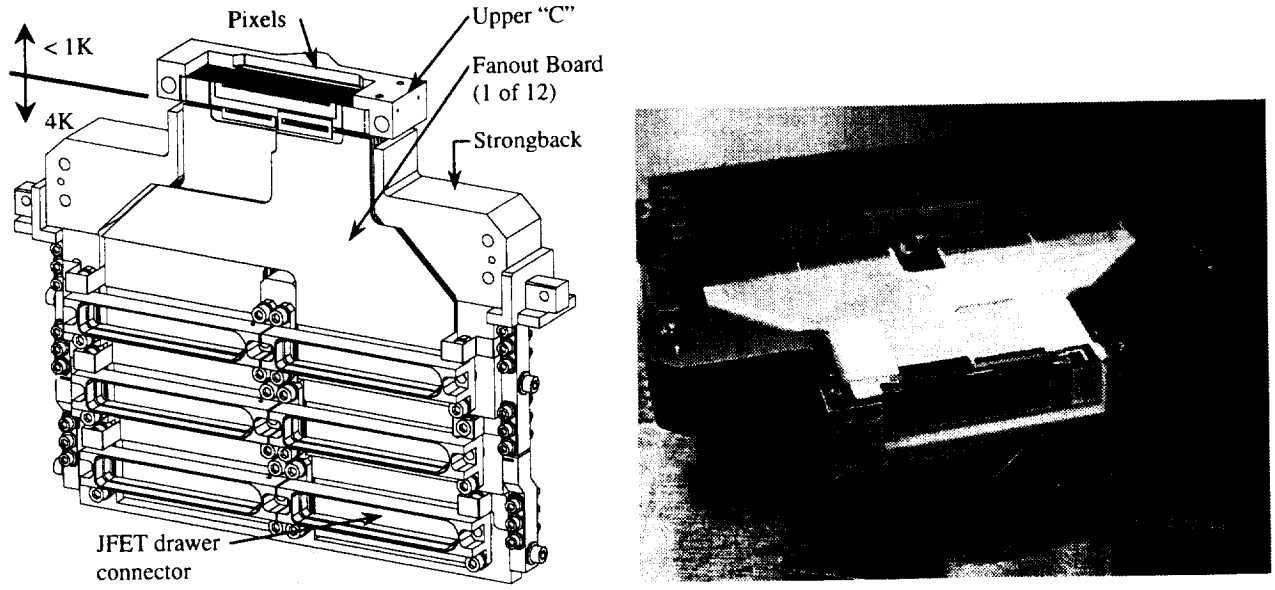

Figures 3&4: Detector core (without JFET drawers or suspension system).

The bulk of the detector operates at 4K. The PUD bolometer assembly operates at either 200 mK (HAWC) or 300 mK (SHARC), which is why the Kevlar suspension is needed. The JFETs operate at 120K, only six inches away from the bolometers, so thermal isolation and radiation blocking are critical design features.

2.1 PUD array folding

The most unique feature of these detectors is the folding of the semiconductor bolometers [3]. This is the key innovation which enables an absorber to abut its neighbors on 4 sides with only a few percent of the collecting area unfilled.

More detail about the bolometer fabrication can be found in [4], but briefly, the PUDs (Fig. 5) are manufactured in 32-element, planar rows using MEMS semiconductor etching techniques. Instead of the usual, straight legs attaching the absorber to the frame, PUDs have a torsional yoke attachment, visible in Figure 6. When the frame of the bolometer is cut as shown in Figure 5, and the two sides of the frame are folded together, the torsional section twists and allows the legs to fold under the absorber, forming a table-like structure (Fig. 6). This allows adjacent rows to be packaged very close together (Fig. 7).

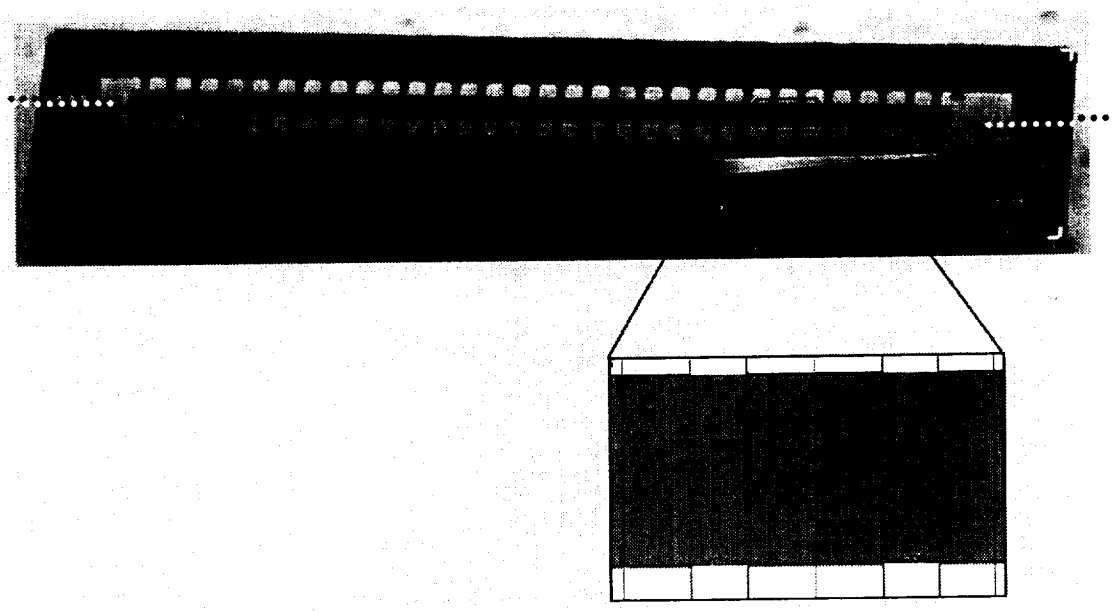

Figure 5: Unfolded PUD array showing cut lines and detail of two pixels.

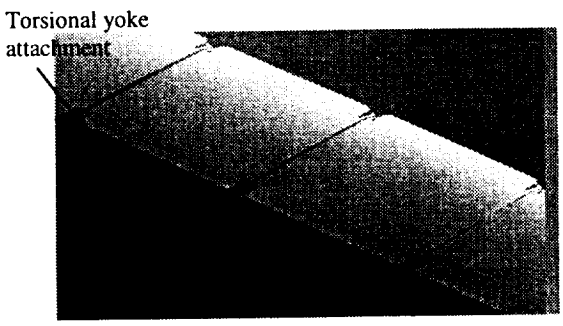

Figure 6: Folded PUD array

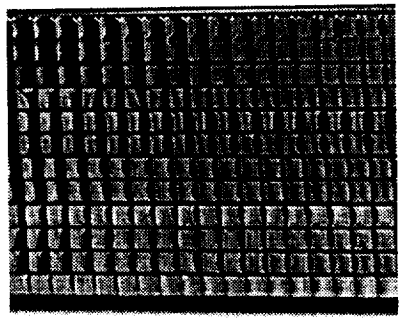

Figure 7: Close-packed 2-D array of folded PUDs - SHARC II (seen face-on)

The cut ends of the frame are glued to a copper plated ceramic thermal bus bar with a very thin film of Epon 815C resin and Versamid 140 hardener, mixed 3:2 [5], which provides a good connection to the thermal sink. Optical alignment during the two-step gluing operation using specialized jigs (Figs.8&9) ensures their uniformity and correct placement.

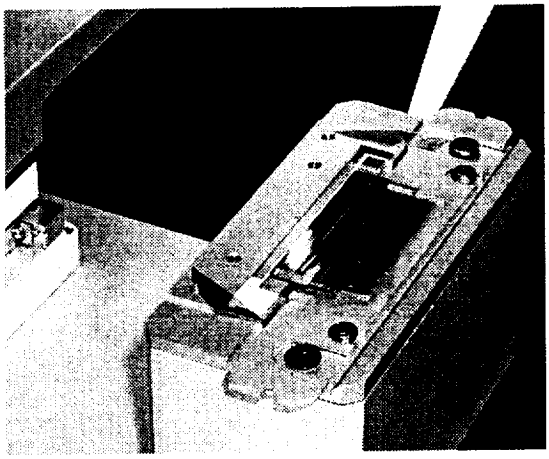

Figure 8: Unfolded PUD in folding jig.

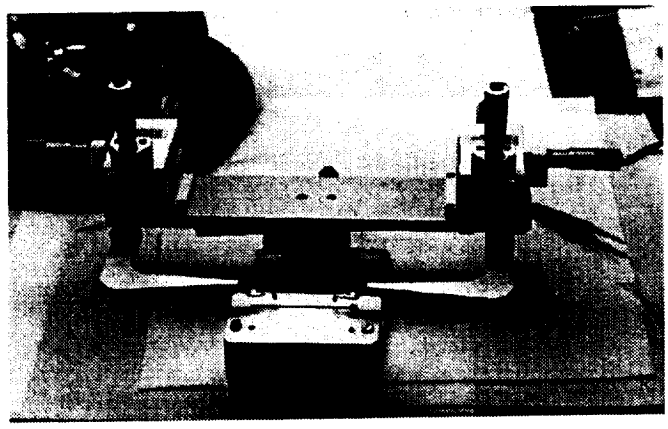

Fig. 9: PUD Alignment Jig

Directly beneath the absorber, the top of the bus bar widens out to almost the same size as the absorber (Fig. 10). Since SHARC-II is optimized for 350 and 450 μm, both of which could be well absorbed by a single resonant cavity tuned to 400 μm, the reflective gold plating was left exposed, and forms a ¼ wave backshort when the absorber is placed 100 μm above it. Getting this gap within tolerance reliably was the single hardest procedure on the detector assembly. As the HAWC detector is a broadband instrument, covering wavelengths from 40 - 300 μm, a single resonant cavity behind the absorber would not work well over the entire wavelength range, so this top surface will be painted IR black [6], and it will serve to absorb the radiation which passes through the bismuth absorber on the bolometer.

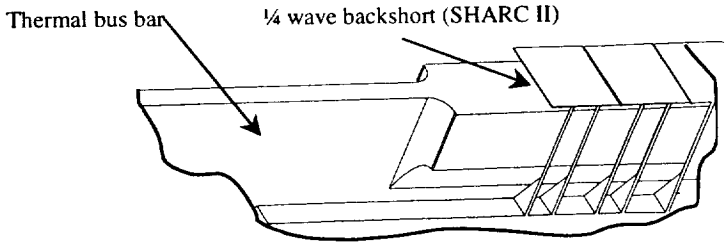

Figure 10: PUDs and thermal bus bar backshort.

This difference between the absorber backshorts is the principal mechanical difference between the SHARC and HAWC detectors.

2.2 Fanning out the signals

In the assembled detector, the PUD/bus bar assemblies will be stacked one above the other. The center-to-center pitch of the pixels was set at 1000 μm. The absorber area was made slightly smaller than the pixel pitch, to allow for small variations in the folding. This pitch was chosen as the best compromise between the competing constraints of final detector array size, required optics focal lengths for nyquist sampling, and feasibility of packaging. This dimension sets the scale of the mechanical package: all the mechanical support and electrical connections for a given PUD row had to fit completely behind that row. The rows and their connections are then stacked up to build the two-dimensional array.

The stacking arrangement is shown in Fig. 11. Alumina ceramic was chosen as the bus bar material because of its close thermal expansion match to the silicon PUDs that are glued to it. To have adequate strength, the bus bar needed to be at least .25 mm (.010") thick. For heat sinking the bolometer frames, we used .05 mm (.002") thick copper plating on both contact surfaces of the bus bar. We gave this a thin flash of gold to inhibit corrosion and improve the thermal contact downstream. The silicon frames themselves are .30 mm (.012") and we allowed for .038 mm (.0015") thick glue lines. A minimum of .38 mm (.015") vertical clearance is required to accommodate the wirebonds which electrically connect the bolometers to the outside world.

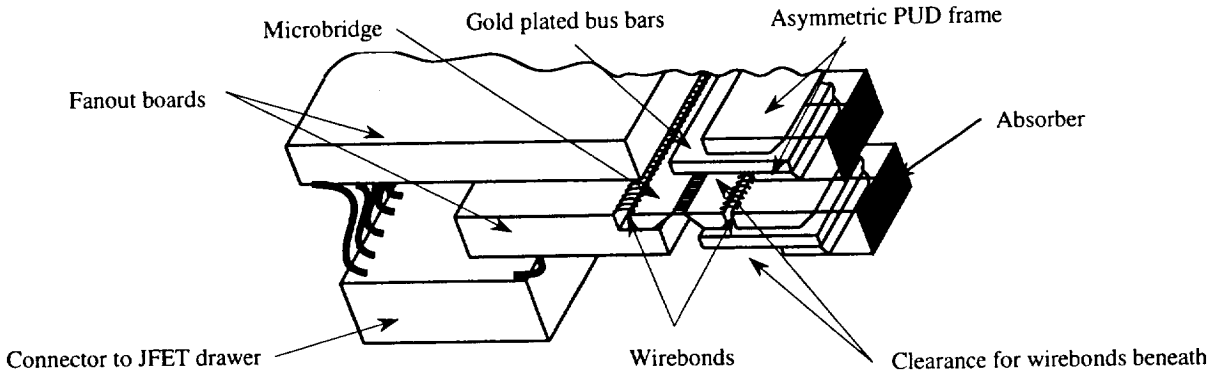

Figure 11: Stacking arrangement.

To help accommodate the wirebonds, the PUD frames are asymmetric, as can be seen in Figures 5&11. When the sides of the frame are cut and it is folded over a bus bar, the side with the wire bond pads extends further than the side without them. Thus, when the next row is laid on top, a small additional space is left above the wirebond pads.

2.3 Detector core assembly

When the detector is complete, a Kevlar suspension system mechanically connects the bolometers to the main detector structure. During the buildup, however, temporary alignment bars maintain proper positioning between the upper C and the strongback (Fig. 12). A PUD/bus bar assembly, prepared as described in the previous section, is glued into the ceramic upper C using Epon/Versamid. One ceramic fanout board is glued into the titanium strongback for each row of PUDs. Silicon microbridges [7](Figs. 11&13) are used to make electrical contact between the cold PUDs and the warmer fanout boards with a minimum of thermal conduction. A microbridge chip is glued in position to interconnect the PUD and the fanout board, the wirebonds are made, and the frame of the microbridge chip is cut, completing the thermal isolation.

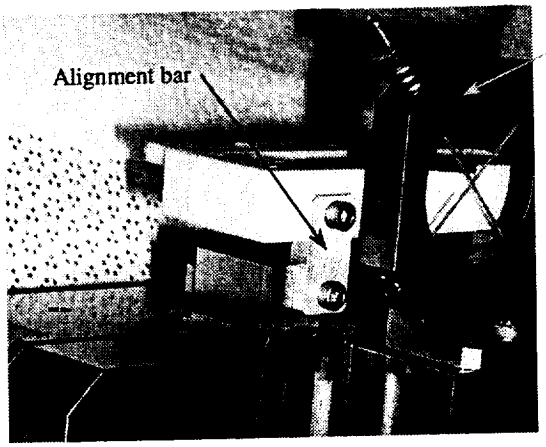

Figure 12: Temporary alignment bars hold the cold stage in position prior to suspension system gluing

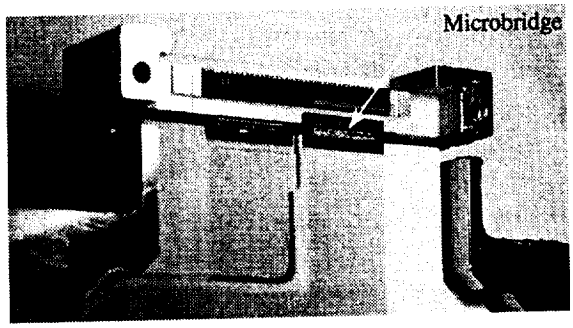

Figure 13: The electrical connections are made across temperature stages using microbridges. Connections are staggered left and right on successive layers.

As the rows of PUDs are stacked up, corresponding bond pads on the PUDs and on the fanout boards, as well as the microbridges which interconnect them, are staggered left and right on successive layers to give more headroom for the wirebonds on the fanout boards (Fig. 13). By leaving room in this way, the fanout boards could be made thicker and stronger. The fanout boards are also alumina, for a good CTE match to the bridge chips which are glued to them.

The lower end of the fanout boards is where the connectors are soldered in place. The detector has 12 bolometer rows and 3 JFET drawers, so each connector has to make contact with 4 fanout boards. As the fanout boards are each behind its own PUD row, they are at 4 different heights, 1 mm apart. We used large, dense connectors from Packard-Hughes (now Delphi Connection Systems)[8] with long, flexible solder contacts, which we bent to reach the different levels of the fanout boards (Figs. 4 & 11). These connectors are anchored to the strongback to prevent mating forces from bending the solder leads.

2.4 Thermal isolation system

Two thermal isolation systems were required for this detector: between the bolometer stage and the main structure, and between the JFET boards and the surrounding JFET drawer.

The base of the PUD bolometers needs to be kept at 200 mK for HAWC and 300 mK for SHARC. We wanted a very low thermal conductivity mount from this cold stage to the rest of the 4K detector for two reasons: to minimize the load on the cold stage refrigerators, and to isolate the PUD bases from fluctuations in the helium bath temperature. We chose to make a tensile structure out of unbraided, 2160 denier, type 968, Kevlar 49 cord because of its low conductivity (2×10^{-4} W/cm·K at 4K) [9] and high stiffness (112 GPa @ room temp)[10].The Kevlar cord is glued into fittings using Stycast 2850 with 24LV catalyst[11]. The lower fitting fits into a matching recess in the suspension tower (Fig. 12), which rigidly constrains the cord. The Kevlar cord crosses the open part of the tower and the upper fitting protrudes from the top side of the tower, where a compression spring and nut are used to preload the cord (Figs. 1 & 12). Two cords are fitted to each of three towers in this fashion. The cold stage is glued at each of the three points where the cords cross, with a drop of Stycast.

An individual preloaded cord is stiff along its length as long as the preload is not exceeded, but relatively soft in the orthogonal directions. A pair of crossed cords in a tower is stiff in the plane of the cords, but is soft normal to this plane and in all three rotation axes. Placing three of these Kevlar tower assemblies at roughly 120 degrees yields a kinematic attachment between the bolometer stage and the rest of the detector. This is desirable to prevent stress buildup, and to prevent lateral shifting of the center of the detector array, during cooldown.

With the cold stage isolated in this fashion, the power from the 4 K stage to the 300 mK stage (for SHARC) was only 4 μW, feeding in from the Kevlar cords and the microbridges. The bus bars were connected to the 200 or 300 mK refrigerator as follows (Fig. 1): a copper foil was glued to the copper plating on the bus bar using Epon/Versamid, mixing in 70 percent by weight silver powder, to make a conductive epoxy. The other end of the foil was clamped to a copper bar. This bar had features to form a labyrinth seal where it penetrated the stray light baffles (Fig. 1), which, while avoiding contact with the 4K baffle, prevented light from entering the PUD vicinity. A flexible copper braid for attachment to the refrigerator is silver brazed into a hole at the end of the bar. This clamps to the heat strap coming from the Adiabatic Demagnetization Refrigerator (ADR) for HAWC or the ^{3}He refrigerator for SHARC.

The JFETs must be heated to 120K to minimize their thermal voltage noise, and the total power (heaters plus JFET dissipation) should be at most on the order of 200 mW, to keep the helium boiloff to 1 fill / day. The approximately 400 microbridge interconnects to each JFET board were estimated to conduct about 2 mW, and radiative losses for each of the three JFET warm boards were expected to be about 15 mW. The maximum thermal gradients along the cold board were set by the need to keep the load resistors adjacent to the JFET board below 8 K to minimize their thermal noise. These parameters determined the allowable thermal conductance of the structural support linking the warm and cold boards, which consisted of a pair of 6.3 mm (.25") long, 6.3 mm diameter Vespel® SP-1 tubes with a .13 mm (.004") thick wall (Fig. 14). The heat flow through these standoffs from 120 K to 4.2 K is approximately 14 mW.

2.5 Radiation shielding and heat sinking

Good thermal isolation is half the battle in keeping the unwanted heat from the 120 K JFETs away from the bolometers: it reduces the power injected into the detector to heat the JFET warm board. Good thermal heat sinking and radiation blocking is equally important. Since a perfect seal cannot be accomplished, as the traces will need to penetrate any seal, multiple stages of isolation, radiation blocking, and heat sinking are required.

The JFET drawer structure consists of the warm JFET board mounted to a cold board with Vespel tubes as described above, inside a titanium housing (Fig.14). The fist line of defense against radiation from the JFET board is an opaque, conductive metal barrier around the warm JFET board. The top of this barrier is formed by a the JFET board shield, and the bottom by the copper plating on the ceramic cold board. A labyrinth seal is made between the two by gluing a rectangular frame of gold plated ceramic to the cold board, which meshes with the shield. To avoid shorting out the traces on the cold board, the underside of this seal was not plated. Of course, this is a necessary radiation leak.

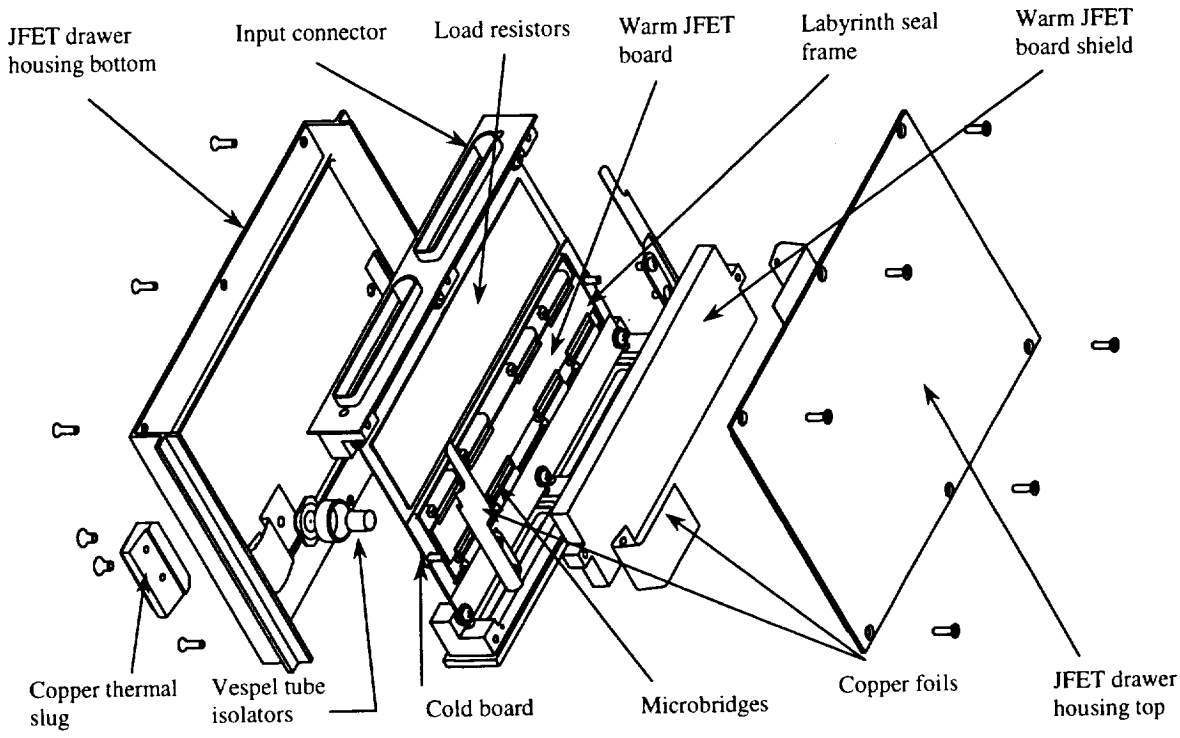

Figure 14: Exploded view of JFET drawer

The warm JFET board cover and the plating on the cold board are well anchored to the helium tank: the titanium housing for the JFET drawer, the second line of defense against JFET radiation, has a copper slug which penetrates through it. The slug provides a good thermal path through the shield, while remaining light-tight. Copper foils, glued to the warm JFET board cover and to the plating on the cold board and then clamped to the inside of the slug, provide a conductive path. Copper ribbons are clamped to the outside of the slug, which are in turn clamped to copper thermal bars that penetrate the JFET box, the third and final radiation barrier. At each radiation barrier penetration, the copper path serves to cool the barrier material. Where the copper thermal bars emerge from the JFET box, they are strapped to the helium tank using copper ribbons or braid.

At the connectors, the electrical traces penetrate the JFET drawer covers, creating a chink in the armor. To fortify this area, aluminized Mylar strips were inserted inside the solder tabs of the connector as a radiation barrier, and the fanout boards had copper foils glued to their backs as a heat sink. Tabs on the foils were clamped to copper bars that penetrated the JFET box enclosure, which were in turn anchored to the helium tank. These foils ensured that the parts of the detector close to the bolometers were as cold as possible.

Finally, a stripe of absorptive epoxy [6]and a last metal radiation baffle at the top of the fanout boards absorb most of the remaining radiation.

3. ENGINEERING RESULTS

The first light run of the SHARC II instrument in April 2002 presented an opportunity to verify the performance of the mechanical design. Our primary concerns were: 1) How many pixels work? 2)How much will the power from the JFETs heat the bolometer frames? and, 3) How much will radiation from the JFETs heat the bolometer absorbers? Our secondary concerns were: 4) Will the load resistors be heated above their 8K thermal noise threshold? 5) Will the fanout boards, carrying the high impedance signals from the PUD array, be susceptible to microphonics? and, 6) How much power are the heaters using to warm the JFETs, and will they boil off too much helium?

1) Out of a maximum possible 384 pixels, 20 pixels were not working. When measured at the connector between the detector core and the JFET drawers, which ignores any problems in the JFET drawers, there were 10 open bolometers. Of these, 4 pixels were known to be mechanically defective prior to their inclusion in the array. Also, there were 16 channel pairs are resistively shorted together (~ 100 kOhm) , probably due to ionic contamination of the ceramic fanout boards. The remaining open channels were due to the JFET drawers. While developing the JFET drawer assembly procedure, a large crack developed in one cold board, severing a third of its traces. Most of these were salvaged with wirebonds and conductive epoxy, but 10 were not repairable and remained open.

2) To measure the heating of the bolometer frames, we compared their temperature with the JFET heaters switched off and on. The temperature went from 306mK to 358 mK, a difference of 52 mK. This was considered acceptable. Additionally, the temperature drop along the conduction path from the PUD frames to the refrigerator was 12 mK with the JFET heaters switched on. These temperatures correlated well with our predictions, and validated all of the choices in conductive glues and plating thicknesses for the thermal path from the bolometers to the refrigerator.

3) To measure the heating of the bolometer absorbers by the JFET heaters, the JFETs could not be switched off, because the bolometer signal could then not be read out. Instead, the heater temperature set point was varied, and the effect on the absorber temperature was measured. Negligible additional power was seen on the bolometers. Additionally, the observed dark NEP of 5x10e-17 $W/(Hz)^{1/2}$ agrees with the prediction for a bolometer with no radiation.

4) With the JFETs powered up, the maximum temperature of the load resistor boards is 7.22 K, so the thermal design was acceptable from that standpoint as well.

5) We obtained a rough indication of the instrument's microphonic susceptibility by rapping on the vacuum shell while the instrument was operating. We saw an increase in the 100 Hz frequency component of the signal which we attributed to the fundamental mode of the entire detector rocking on its flexures. Other than that, vibrations of the detector signal chain had no measurable impact. During observations at the CSO, the signal was not affected by the telescope's motion.

6) Finally, we determined that the additional power required to heat the JFETs to their operational temperature is 30 mW per drawer, and the dewar hold time, with the JFET heaters switched on, exceeds 50 hours.

In summary, the thermal performance of the detector exceeded our requirements in all areas.

4. REFERENCES

1. D. A. Harper et al., "HAWC – a far-infrared camera for SOFIA", Proceedings Of SPIE, Vol. 4014, pp. 43-53, 2000

2. C. D. Dowell et al.," SHARC II: a Caltech submillimeter observatory facility camera with 384 pixels" in Astronomical Telescopes & Instrumentation: Millimeter and Submillimeter Detectors for Astronomy, Thomas G. Phillips, Jonas Zmuidzinas, Editors, Proceedings of SPIE Vol. 4805 (to be published 2002)

3. S.H. Moseley et al.,"Large-format bolometer arrays for far-infrared and submillimeter astronomy" in Astronomical Telescopes & Instrumentation: Millimeter and Submillimeter Detectors for Astronomy, Thomas G. Phillips, Jonas Zmuidzinas, Editors, Proceedings of SPIE Vol. 4805 (to be published 2002)

4. M. J. Li, C.A. Allen, S.A. Gordon, J.L. Kuhn, D.B. Mott, C.K. Stahle, L. L. Wang, "Fabrication of Pop-Up Detector Arrays on Si Wafers", Proceedings Of SPIE Vol. 3874 pp. 442-431, 1999

5. Epon 815 resin: Resolution Performance Products, Houston, TX 77251
   Versamid 140 hardener: Cognis Chemicals, Kankakee, IL, 60901

6. J.J. Bock, "Rocket-borne observation of singly ionized carbon 158 micron emission from the diffuse interstellar medium", PhD Dissertation, California Univ. Berkeley,CA,1994, Physics dept, page 110

7. C.A. Allen, S.H. Moseley, D.S. Schwinger, D.E. Franz, "Low Thermal Conductance Silicon Microwires Fabricated by MEMS Processing for Cryogenic Electrical Interconnects", Nanospace 1998, Houston, Tx

8. High Density Printed Circuit Connector, Delphi Connection Systems, Irvine CA, 92614

9. J.G. Hust, "Low–temperature thermal conductivity of two fibre-epoxy composites", Cryogenics (1975) 15 126 – 128

10. Kevlar® Aramid Fiber Technical Guide, Dupont publication

11. Stycast 2850FT catalyst 24LV: Emerson & Cumming, Billerica, MA 01821